Available online at www.sciencedirect.com
ScienceDirect
Thermochimica Acta 449 (2006) 27–34
thermochimica acta
www.elsevier.com/locate/tca

Assessment of acid–base strength distribution of ion-exchanged montmorillonites through NH_3 and CO_2-TPD measurements

A. Azzouz [a,*], D. Nistor [b], D. Miron [b], A.V. Ursu [b], T. Sajin [b], F. Monette [c], P. Niquette [c], R. Hausler [c]

[a] *Department of Chemistry, University of Quebec at Montreal, H3C 3P8 Canada*
[b] *Catalysis and Microporous Materials Laboratory, Bacau University, RO-5500, Romania*
[c] *STEPPE, École de Technologie Supérieure, Montréal, Québec, H3C 1K3 Canada*

Received 1 May 2006; received in revised form 8 July 2006; accepted 24 July 2006
Available online 31 July 2006

Abstract

Distribution of the acid–base strengths of various ion-exchanged montmorillonites was assessed through thermal programmed desorption (TPD) of NH_3 and CO_2. Accurate acid–base measurements can be achieved via deconvolution of perfectly symmetrical peaks, under optimal carrier gas throughput and heating rate, estimated though a factorial experiment design. No neutral clay samples without interactions with carbon dioxide or ammonia were found. All clay samples displayed both acid and base characters, with specific TPD patterns, and no pure acidic or pure basic clay materials were obtained. Increasing cation radius led to increasing acidity and decreasing basicity, in terms of both total amount of desorbed probe gas and strength of the adsorption sites. It was suggested that basicity and weak acidity are intrinsic features of the clay structure, while medium and strong acidities are induced by the exchangeable cation.

Keywords: Ion exchange; Montmorillonite; TPD; Acidity; Basicity; Strength distribution

1. Introduction

When contacted with gases, clays can behave either as base and/or acid [1,2], resulting in various gas–solid interactions, ranging from mere physical retention to strong chemical adsorption. Such interactions, particularly those occurring between soils and atmospheric pollutants, are strongly dependent of both the area and chemical composition of that part of the surface accessible to gases. Recently, major concerns have been focused towards the negative effect of acidic or basic gases upon the chemistry of soils, and the way soils react towards air pollution. In this regard, the concepts of acidity and basicity can be very useful to assess the interactions between solid surfaces and gases. Some of these concepts have partially been applied to clay-rich soils [3], and can be of essential importance for environmental chemistry.

Clays appear to be the most interesting microporous materials in terms of availability, widespread and properties. Nonetheless, so far, no comprehensive approaches were developed for achieving better overview of the nature and magnitude of gas–solid interactions. Clay surfaces display electric charges and modulable electrostatic fields as a result of their ionic structure. Through suitable modifications, clays have found diverse applications [4–8], being regarded not only as effective ion-exchangers, pH-modifying agents, but also as effective gas-adsorbing agents. Some authors [8] claimed that the mere presence of a clay material favors retention of carbon dioxide, and that acid treatment improves the retention capacity of the material. This result was explained in terms of increasing numbers of Brønsted and potential Lewis acid sites, as long as the clay structure is preserved under acid attack. Nonetheless, no uses of crude untreated clay-rich materials for gas retention purposes have been envisaged so far.

Assessment of the acid–base character of clays could be of greatest importance in providing us with information upon how clay-rich materials can selectively fix or release gases present in surrounding atmospheres. This is why the present study

* Corresponding author. Tel.: +1 514 9873000; fax: +1 514 9874054.
E-mail address: azzouz.a@uqam.ca (A. Azzouz).

0040-6031/$ – see front matter © 2006 Elsevier B.V. All rights reserved.
doi:10.1016/j.tca.2006.07.019

has been undertaken through both experimental and theoretical approaches. On one hands, thermal programmed desorption (TPD) attempts were performed on a series of montmorillonite samples ion-exchanged with a wide variety of cations, ranging from alkalines to actinides. Ammonia and carbon dioxide, used herein as probe gases, are supposed to be quite representative to investigate the interactions occurring between clays and base or acidic gases. On the other hands, a mathematical model was also formulated, providing a quick analytical method that enables accurate assessment of the strength distribution of the acid–base properties of the clay samples.

2. Experimental

2.1. Clay preparation and characterization

A montmorillonite-rich material (Mt) having a Si:Al mole ratio of 1.34 [9] was obtained through purification of a smectite clay material (bentonite) originating from Maghnia repository (Algeria), and supplied by ENOF Ltd. (Algeria). The major components are silica (51%), alumina (32%), magnesia (4%), Fe_2O_3 (2.5%), Na_2O (1.5%) and small amounts (less than 1%) of K_2O, CaO and MnO. The native clay contains preponderantly montmorillonite (Mt), in a proportion exceeding 81 wt.%. The mineralogical composition also includes quartz (14 wt.%), cristoballite (4.0 wt.%) and beidellite (less than 1 wt.%).

Thorough purification through ultrasound treatment, acid washing, repeated settling in distilled water, calcinations at 450 °C, ion-exchange and dialysis, according to an optimized technique fully described elsewhere [1,10] provided a 95% pure montmorillonite. The latter was first ion-exchanged into the NaMt form, and then various samples were repeatedly impregnated with saturated aqueous solutions containing nitrate salts of H^+, Na^+, K^+, Ca^+, Mg^{2+}, Cr^{2+}, Mn^{2+}, Fe^{2+}, Co^{2+}, Ni^{2+}, Cu^{2+}, Cd^{2+}, Mo^{3+}, Pb^{2+}, Hg^{2+}, La^{3+}, Ce^{3+}, and $UO_2{}^{2+}$ cations, so as to be fully ion-exchanged into the respective forms. The protonated form, referred to by HMt, was obtained via ion-exchange with aqueous NH_4NO_3 solution, followed by controlled heating at 400 °C to remove ammonia. Ion exchange was carried out under vigorous stirring, for 5–6 h at 80 °C, and repeated three to five times with fresh salt solutions. HMt, NaMt, KMt, MgMt, CaMt, CrMt, MnMt, FeMt, CoMt, NiMt, CuMt, MoMt, CdMt, HgMt, PbMt, LaMt, CeMt and UO_2Mt samples were further dialyzed in hot deionized water (40–50 °C) in order the remove the physically sorbed salt excess, filtered, and air-dried overnight at 25 °C. An average cation exchange capacity (CEC), estimated by measuring the released Na^+ amount through atomic absorption spectrometry, was found to be of 0.95–110 meq/100 g at neutral pH.

The dry clay samples were further characterized through X-rays diffraction (XRD) analysis using a Philips PW 1710 diffractometer with a CuK radiation (λ = 1.54051 Å). The native crude clay material showed a broad 0 0 1 line, due to the wide variety of species sandwiched between the clay sheets. Quartz (identified by the 4.28, 3.36, 2.23, 1.66, 1.54 and 1.37 Å XRD lines) and cristoballite (detected through the 5.34, 4.09 2.50 and 1.38 Å XRD lines) were removed in proportions of ca. 80% after purification. The nearly pure montmorillonite obtained displayed perfectly parallel clay sheets, devoid of any amorphous phases, as indicated by a straight baseline and a sharp 0 0 1-XRD line [1,9].

2.2. Measurements of acidity and basicity

TPD measurements were achieved using N60 pure grade gases. A 200 mg clay sample having a 0.1–0.2 mm particle size, was introduced in the cylindrical glass microreactor (2 mm internal diameter) of the TPD device so as to obtain a 2–3 cm height fixed clay-bed, which is then dried at 400 °C for 5–6 h under a nitrogen flow, at normal pressure. Such operations conditions are essential requirements for achieving adsorption–desorption equilibrium and to prevent from diffusion hindrance. The clay sample was further cooled up to the injection temperature: 80 °C for CO_2-TPD or 120 °C for NH_3-TPD. Carbon dioxide or ammonia was injected through the clay fixed bed till saturation, and the excess of the probe gas was purged at the respective temperature. Saturation is attained when no more absorption is observed, and the inlet and outlet amounts of the probe gas are balanced, or in other words when the amount of probe gas injected in the TPD microreactor is equal to that of the probe gas evacuated into the titration device.

Preliminary experiments were performed with various carrier gas throughputs ranging from 20 to 120 mL min^{-1} for optimization purposes. The results presented herein arise from 3^3 factorial experiment designs achieved by varying simultaneously three parameters, namely: the heating rate (X1), gas throughput (X2) and the particle size (X3), as summarized in Table 1. For the sake of brevity, the entire procedure and calculations were not presented in the present manuscript.

The value of 80 mL min^{-1} was found to be optimal for the adsorption–desorption equilibrium to take place, at the fixed heating rates and particle size, preventing from forced desorption of the probe gas molecules. Later, CO_2-TPD was achieved with a constant heating rate of 70 °C h^{-1} in the temperature

Table 1
Levels of key-parameters for 3^3 factorial design for optimization of the operating conditions

Parameter	Symbol of coded parameter	Minimum value (−1)[a]	Medium value (0)[a]	Maximum value (+1)[a]
Height of the clay bed (cm)	x_1	0.5	3.25	6
Particle size (mm)	x_2	0.05	0.25–0.26	0.5
Gas throughput (mL min^{-1})	x_3	20	50	120

[a] In parenthesis: coded variable, i.e. the corresponding reduced (non-dimensional) parameter value. The response function was the peak resolution, arbitrarly expressed in terms of maximum distance between two peaks summits. Peak width was also taken into account as qualitative criterion.

range of 80–500 °C, while NH_3-TPD was performed with a constant heating rate of ca. 75 °C h^{-1} in the temperature range of 120–550 °C. The desorbed probe gas was evacuated by the carrier gas was bubbled during 15–18 min in 2 mL samples of a 0.02 N sulfuric acid solution or NaOH, through a 2 mm × 20 mm cylindrical porous glass bubbler and determinated by back titration using a 0.01 N NaOH or H_2SO_4 solution. The solution excess was back titrated by potentiometry. To avoid contact with external air and measurement errors, the sampling and titration operations were carried out using a semi-automatic sealed device filled with pure nitrogen.

Acidity and basicity were estimated as being the total amount of NH_3 or CO_2 released through thermal programmed desorption (TPD) per gram of dry clay sample, inasmuch as the number of desorbed molecules is supposed to be equal to that of the adsorption sites present on the clay surface. The acid or base strength will be proportional to the temperature required to release the probe gas molecules. The strength distributions were expressed in terms of various amounts of ammonia or carbon dioxide desorbed under controlled temperature increase, and were estimated by TPD pattern deconvolution [11]. For the sake of accuracy, preliminary TPD measurements were performed on pure standard [quartz + cristoballite] mixtures. As expected [1], the effect of the remaining traces of quartz and cristoballite on the strength distribution was found to be negligible.

Additional stepwise thermal desorption attempts (STD) were performed through step-by-step heating program with a heating rate stages of 7–10 °C min^{-1} between two consecutive temperature. STD requires longer analysis times than TPD, but provides valuable data when peak resolution or precise acid:base measurements are needed.

3. Results

3.1. Acid–base character induced by ion exchange

A large series of NH_3-TPD measurements were performed on clays samples modified with a wide variety of exchangeable cations, some of them being presented in Fig. 1. The results

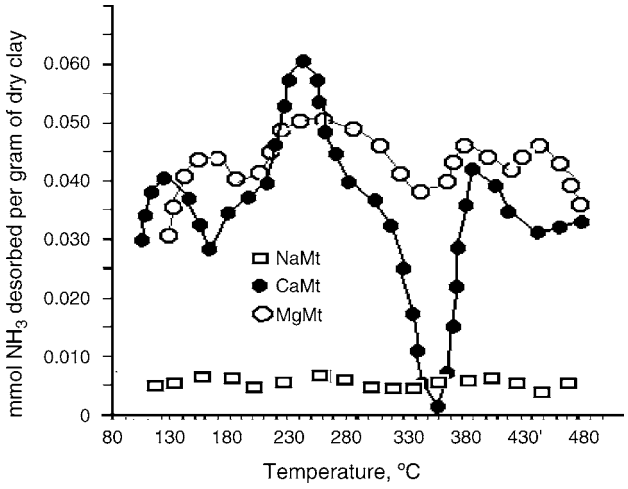

Fig. 1. NH_3-TPD patterns of some ion-exchanged clays.

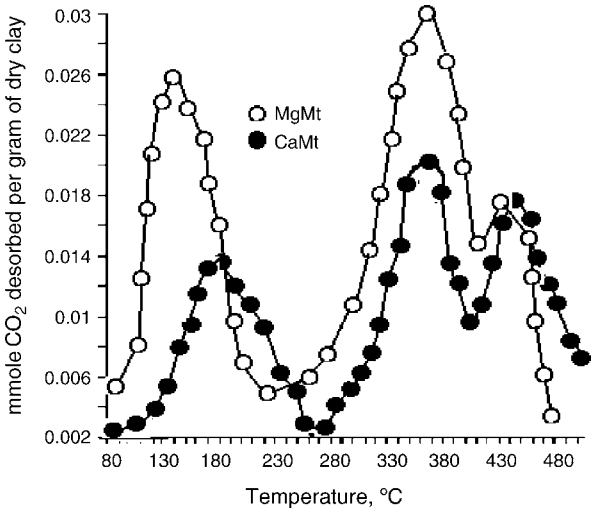

Fig. 2. CO_2-TPD patterns of alkaline earth exchanged clays.

presented herein provide evidence that ion exchange induces specific changes in the acid character for each exchanged clay, in agreements with previous data [1]. Most of these TPD patterns show three desorption peaks that differ from a sample to another by their positions, heights and widths, indicating changes not only in the total acidity, expressed in terms of millimoles NH_3 desorbed per gram of dry clay, but also in the distribution of the acid strength.

Similarly, basicity measurements through CO_2-TPD showed that carbon dioxide also reacts differently with various clay samples (Fig. 2). Nearly similar number of desorption peaks as for ammonia was observed.

As a general feature, all samples displayed simultaneously acid and base character, regardless to the cation introduced by ion exchange. Moreover, it appears that there no exist inert clay materials that do not react with ammonia or carbon dioxide. The consequences of this statement could be of a great interest for environmental researches.

Calculations of the entire area limited by the TPD curve show that ion-exchange with various cations, ranging from alkaline

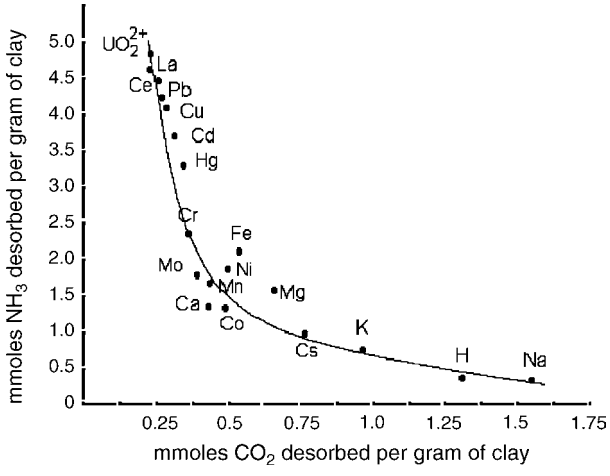

Fig. 3. Total acidity and basicity of the exchanged clay according to the cation introduced.

to actinides, induced an increase of the total acidity from 0.5 to 4.5 mmol NH_3 desorbed per gram of clay. Simultaneously, a decrease of the total basicity from ca. 1.6 to 0.25 mmol CO_2 desorbed per gram of clay was registered, as illustrated by Fig. 3. In agreement with previously reported data [12–15], the general tendency is that acidity increases while basicity decreases, suggesting similarity with aqueous media.

Hereafter, according to the above observations, some findings may already be stated, namely: (i) it seems that there is no pure acidic or pure base clay materials, and all clays must possess simultaneously both acidic and base sites, whatever the charge compensating cation may be; (ii) both acidity and basicity vary according to the exchangeable cation; (iii) acidity appears to be inversely proportional to basicity.

3.2. Correlation between the heating rate and the gas flow rate

In many cases, peak overlapping makes difficult the accurate assessment of the acid or base strength distribution, and peak separation becomes strongly recommended. For this purpose, several STD analyses with CO_2 and NH_3 were performed by increasing temperature from 100 to 550 °C with three temperature stages at 250, 450 and 550 °C. At each step, temperature was maintained constant till the total peak elution, and was increased once again up to the next stage, and so forth. For the sake of brevity, only the CO_2-STD pattern of Mg–Mt is presented herein in Fig. 4.

Comparison with the corresponding CO_2-TPD pattern of Mg–Mt already presented in Fig. 2 provides clear evidence that there exists a narrow analogy between TPD and gas chromatography [16,17]. A specific feature of TPD is that peaks elution evolves with increasing temperature.

Additional demonstration of such a statement can be achieved through a suitable modeling that supposes that the tubular TPD reactor will behave as a package-free open column, and the fixed bed of clay sample will merely be regarded as an injection chamber. One also assumes that no competitive adsorption of nitrogen takes place. In these conditions, the global mass-balance equation for both the gas phase (mobile phase) and clay bed, on an infinitesimal length dx of the column, will be expressed as follows [17–20]:

$$D\frac{\partial^2 C}{\partial x^2} = v_x\frac{\partial C}{\partial x} + \frac{\partial C}{\partial t}(1+k) \tag{1}$$

where

$$C = C_{\text{gas}} + C_{\text{Clay}} \tag{2}$$

$$D = D_{\text{gas}} + kD_{\text{Clay}} \tag{3}$$

$$C_{\text{Clay}} = k(T)C_{\text{gas}} \tag{4}$$

and C_{gas} is the concentration of desorbed probe gas in the mobile gas phase, C_{clay} the concentration of adsorbed probe gas on the clay, D_{gas} the diffusion coefficient of the probe gas in the mobile gas phase, D_{clay} the diffusion coefficient of the probe gas on the clay and $k(T)$ is the partition constant (adsorption constant).

$k(T)$, the adsorption constant, strongly depends on the pK_a or the pK_b of the acid or base sites. In optimal operating conditions, no convection and no re-adsorption take place [20], and, hence, desorption will involve only diffusion. If D_{eff} is defined as being the effective diffusion coefficient and v_{eff} the effective linear gas velocity through the desorption column:

$$D_{\text{eff}} = \frac{D_{\text{gas}} + kD_{\text{Clay}}}{1+k} = \frac{D}{1+k} \tag{5}$$

$$v_{\text{eff}} = \frac{v_x}{1+k} \tag{6}$$

it results that, a particular solution to Eq. (1) can be obtained by Laplace method of integration [21,22], namely:

$$C(x,t) = \frac{a}{\sqrt{4\pi D_{\text{eff}}t}}\,\mathrm{e}^{-(1/2D_{\text{eff}}t)((x-v_{\text{eff}}t)^2/2)} \tag{7}$$

Eq. (7) is viewed as a conventional column-profile for a fixed temperature, expressed as a function of x, the column axis coordinate, that describes a Gaussian-shaped peak having a $v_{\text{eff}}t$ mean and a $2D_{\text{eff}}t$ variance. At constant flow rate of the carrier gas, each peak will move with a constant velocity v_{eff} through the column.

With controlled increasing temperature, desorption is supposed to occur unidirectionally, along the column axis [17], like in programmed temperature gas chromatography [23], and to a lesser extent like in thermal differential analysis [24]. For given acid or base strength, desorption is governed by fixed pK values of the surface. Thus, the adsorption constant, and subsequently, the partition capacity (from Eq. (4)) will be considered as being constant in a relatively narrow temperature range of each TPD peak that does not exceed 200 °C. When no forced desorption occurs, the time needed for thermal desorption will be equal to that required by the desorbed molecules to move along the column:

$$t = \frac{x}{v_x} = \frac{T}{r_{\text{T}}} \tag{8}$$

This makes desorption to take place only upon heating without convection, and it becomes thus possible to replace time and x, the column length coordinate by temperature, and v_x, the gas

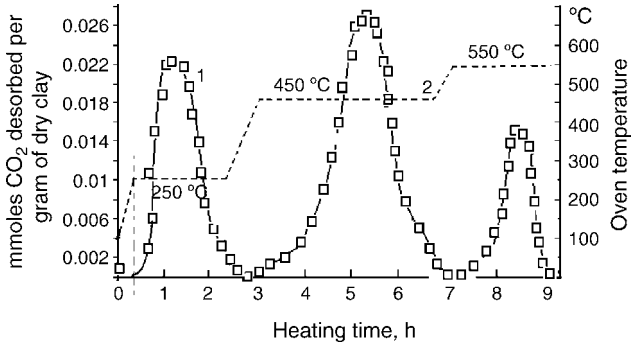

Fig. 4. Stepwise thermal programmed desorption diagram of CO_2 over Mg-exchanged clay at a programmed variation of the heating rate. (1) Desorption curve and (2) heating curve (dashed line).

linear velocity:

$$v_x = \frac{Q_v}{A_{eff}} = \frac{x}{t} \quad (9)$$

which are maintained constant during TPD experiments. Q_v is the volume throughput of the carrier gas and A_{eff} is the effective area of the column cross-section, which depends on porosity and the clay particle size. The resulting concentration profile is expressed as a function of temperature [23]:

$$C(T) = \frac{a}{\sigma\sqrt{2\pi}} e^{-(1/\sigma^2)(Q_v/r_T A_{eff})(k/(1+k))^2(T^2/2)} \quad (10)$$

where

$$\sigma = \sqrt{2D_{eff}\frac{T}{r_T}} \quad (11)$$

To be perfectly symmetrical, the peak skew, defined as being the third zero-point moment, must be equal to zero [16,17]. This corresponds to:

$$\frac{Q_v}{r_T A_{eff}}\left(\frac{k}{1+k}\right) = 1 \quad (12)$$

and needs to satisfy two conditions, namely: (i) for non-neutral acidic of base sites, one has always $k \gg 1$, and the probe gas molecules are retained and need heating to be released. It results, for a given particle size (A_{eff} fixed); (ii) the linear velocity of the probe gas molecules must be set according to the heating rate. Only in these conditions, calculations fit well the experimental measurements as illustrated by Fig. 5, and TPD peaks can easily be deconvoluted. Therefore, any shoulder or even any slight asymmetry will presumably correspond to overlapped peaks (peaks 2 and 3 in Fig. 5).

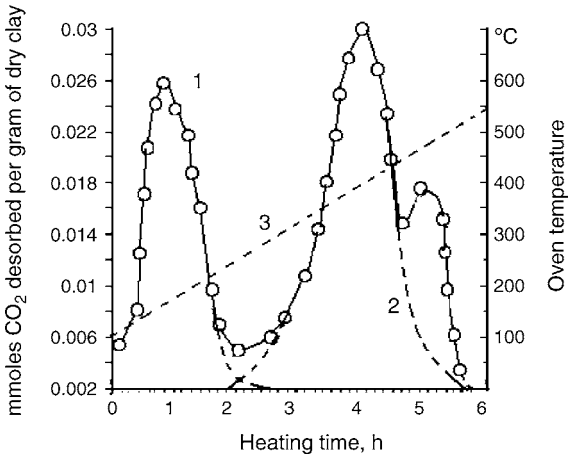

Fig. 5. Method for peak deconvolution through Gauss model for CO_2-TPD pattern of Mg–Mt sample at a constant heating rate. (1) Experimental curve; (2) calculated curve; (3) heating curve.

To achieve analogy between TPD and an axial diffusion in a non-ideal linear equilibrium gas chromatography [16], the probe gas molecules must have laminar flow, by choosing adequate heating rate and particle size. For the sake of accuracy, a series of additional TPD measurements were performed by varying the gas flow rate, the heating rate and the clay particle size according to 3^3 experiment factorial design. An optimal flow rate of the carrier gas not exceeding 80 mL min^{-1}, was determined for a 0.1–0.2 mm particle size, and a heating rate of ca. 75 °C h^{-1} for NH_3-TPD, or 70 °C h^{-1} for CO_2-TPD. One also observed that

Table 2
Distribution of the strength of acidity via NH_3-TPD and basicity via CO_2-TPD

Sample	Acid strength distribution (peak area %)[a]				Base strength distribution (peak area %)[a]			
	Weak (100–200)	Medium (200–300)	Strong (300–400)	Very strong (400–500)	Very weak (80–250)	Weak (250–380)	Medium (380–450)	Strong (450–550)
HMt	6	50	40	7	35	30	25	10
NaMt	50	40	10	0[b]	30	35	20	15
KMt	48	42	10	0[b]	40	33	12	15
MgMt	15	40	20	25	36	48	10	6
CaMt	12	46	18	24	30	45	20	5
CrMt	10	27	25	38	55	23	17	5
MnMt	15	25	35	25	49	28	20	3[b]
FeMt	2	30	25	43	45	28	20	7
CoMt	15	39	34	12	40	35	10	15
NiMt	26	25	27	22	31	36	28	5
CuMt	10	35	35	20	45	26	24	5
MoMt	30	15	25	30	32	40	20	8
CdMt	10	30	35	25	35	5	45	15
HgMt	12	30	37	25	35	40	18	7
PbMt	5	40	30	25	44	16	30	10
LaMt	5	30	35	30	45	25	25	5
CeMt	2	31	37	30	47	29	18	6
(UO_2^{2+})Mt	3	25	37	35	54	34	10	2[b]

Because various clay samples present different T_{max} values in each temperature range, for comparison, the data summarized in this table were assessed by calculating common surface areas defined between two vertical lines corresponding to the temperature range limits, even if there is no peak summit in the respective range.

[a] Relative error: 5%.

[b] The values smaller than 5% are regarded as being negligible, taking into account the value of the accuracy in estimating the strength distribution for both the acid and base properties.

higher flow rates affect the peak symmetry, while below this optimal value, the shape of the TPD pattern does not seem to change, whatever temperature may be.

Thus, one has demonstrated the narrow dependence occurring between the flow rate of the carrier gas and the heating rate for a given porosity (or particle size) in the fixed bed. The assessment of a peak area will only need to determine graphically the height and the half peak width.

Thus, integration of a peak area does not require the baseline to attain zero, but will only need to assume that the peak shape obeys Gauss model, and to known few key-measurements, among which the suspected position of the peak maximum. When such measurements are difficult to achieve, one must additionally assume that any peak asymmetry will be regarded as the sum of at least two parts of peak areas, and further through suitable calculations using only four points (measurements) from the suspected common line belonging to the suspected overlapped peaks, it is possible to obtain a linear system of four equations with four unknown variables (namely two peaks heights and two peak widths).

3.3. Distribution of the acid and base strengths

Measurements of the peak areas were achieved with a 5% error arising mainly from the acid–base titration of the desorbed probe gas, and the results are summarized in Table 2. However, this error it is sufficiently small to afford acceptable average strength distribution for each cation family.

It appears that the acid strength increases but the base strength decreases with increasing atomic mass of the exchangeable cation, confirming, once again, the reverse proportionality between the acid and base character for each clay material (Figs. 6 and 7).

As a general feature, alkaline cations induced predominantly medium and weak acid strength on the clay surface in a proportion of ca. 90%. This agrees with their low hydration grade and small polarizing effect [13]. Rare earths and uranyl cations promote instead medium to very strong acid strengths in a proportion exceeding 95%. Between these two limits the total acidity and acid strength increases progressively in the same

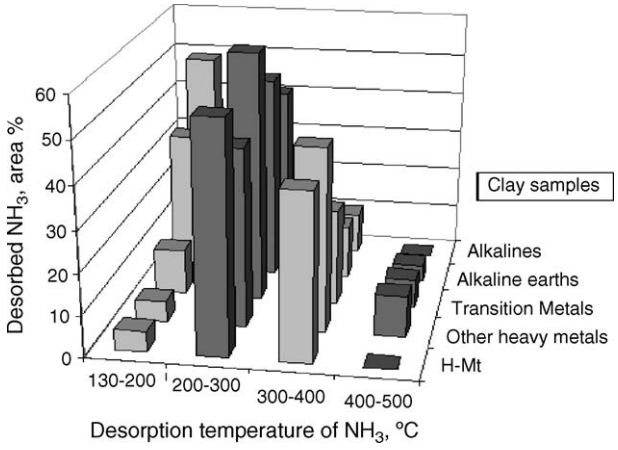

Fig. 6. Acid strength distribution according to the cation introduced.

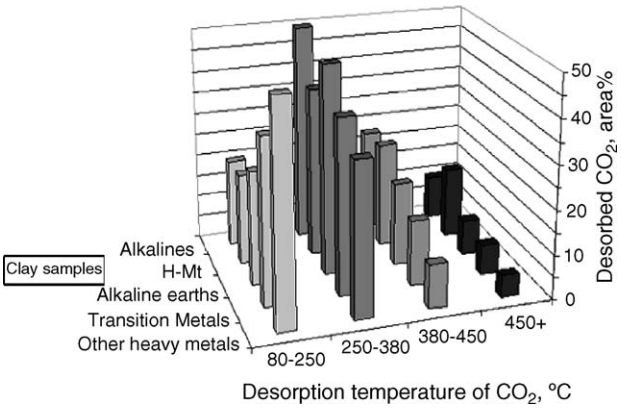

Fig. 7. Base strength distribution according to the cation introduced.

following sequence:

$$\text{Alkaline} < \text{alkaline earths} < \text{transition metals} < Mo^{3+} < Cd^{3+} < Hg^{2+} < Pb^{2+} < La^{3+} \sim Ce^{3+} < UO_2^{2+}$$

In the meantime, the proportion of weak base sites increased from ca. 20 to approximately 50% from alkaline to heavy elements, and the base strength decreased subsequently, in the reverse sequence. At the limit, the base strength that can be shaded by the acid character of strongly acidic clays [14,25]. It results that there no exists pure acidic clays without base properties, and vice versa. Even the HMt sample cannot be regarded as pure acidic material, because three CO_2-TPD peaks were also observed at 80–240, 240–380 and 380–460 °C. This base character may arise unavoidably from the oxygen atoms surrounding the respective cations, but with weaker strength as compared to alkali-exchanged clays, as already asserted by some authors [26].

One must also underline that the strength distribution does not undergo significant changes under repeated calcinations up to 500 °C and rehydrations, except for UO_2^{2+}-containing clay, because partial conversions of uranyl cations into U_2O_3 and (or) UO_2 unavoidably occur in the presence of traces of nitrate anions [15].

4. Discussion

4.1. Acid–base interactions between solids and gases

A wide variety of materials like zeolites and clays can fix ammonia or carbon dioxide, and display acid–base properties. Acid-treated smectites, layered double hydroxides (LDH) and aluminosilicate xerogels (ASG) have already shown affinity in retaining CO_2 [8,27,28]. When clays were contacted with CO_2, their interactions with gases were explained in terms of changes in the numbers of Brønsted and potential Lewis acid sites, as long as the clay structure is preserved under acid attack [8]. Some authors assert that only the chemically adsorbed ammonia corresponds to the solid acidity [27]. This assertion does not agree with our experiments, since the amount of released probe gas is always higher than that of the expected number of adsorption site on the clay surface. Therefore, the acid–base character

may also involve pure physical attractive forces between the material surface and the surrounding gas molecules. Some of these physical retentions of ammonia are mainly due to terminal silanol and aluminol groups, which effectively contribute to the acid–base character of clay material, and cannot be ignored. If one assumes that any acidity on the clay surface may influence the basicity of the surrounding oxygen atoms, one must expect that the latter will exert a wide variety of attraction strength towards carbon dioxide ranging from chemical interactions to pure physical retentions.

A question that still remains to be answered is whether protonation and deprotonation of the clay surface take place in dry media, as in polar solvents. If the adsorbed probe gas molecules behave like a solvent, one must expect that Brønsted acidity will require strong polarities. Nitrogen, used as herein as carrier gas, like any other non-polar molecules may also adsorb on the clay surface, at room temperature, as already stated by some authors [29,30]. Gas adsorption cannot be attributed only to ion–quadrupole interactions with the clay surface, as already stated [29,31], because such interactions may not play significant role with increasing temperature. For instance, carbon dioxide is also a non-polar molecule but exhibits stronger interactions with the clay surface than nitrogen, presumably due to chemical formation of carbonate species with the framework oxygen's, like in limestone. The amount of released carbon dioxide does not seems to be greatly affect by ion-exchange, suggesting a certain stoichiometry, but the base strength is strongly dependent on ion-exchange. That is, it appears that basicity on cationic clays is exclusively of Lewis nature. Ammonia also reacts with protonated acid sites, generating ammonium groups on the clay surface. The different amounts of desorbed ammonia measured for various clay samples indicates that acidity is partly of Brønsted type, and must necessarily depend on some properties of the exchangeable cation, most likely the polarizing effect and hydration grade [29].

4.2. Effect of the exchangeable cation

On a given clay, the terminal aluminol and silanol groups located at the edges of the clays sheets exhibit an intrinsic weak acidity. This acidity is not greatly influenced by ion exchange and corresponds to the first peak in a TPD pattern. The surrounding framework oxygen's are expected to display base character. Changes in the chemical composition induced by the exchangeable cation on the host surface modify the acid–base distribution. For instance, low hydrated cations like alkalines are known to induce Lewis basicity on the negative charge of oxygen atoms surrounding the exchangeable cation [1,25]. Small fluctuations of this intrinsic Lewis basicity also occur according to the cation [12–14]. Unlike the data provided by some authors [30], alkaline earth-exchanged clays also exhibited base character, in agreement with previously reported results [26–30], but of slightly weaker strength, as compared with alkali-exchanged clays.

In contrast, ion exchange with heavier cations promotes mainly Brønsted acid sites, which release strong acidic protons upon water hydrolysis within the $[([Clay]^{n-})Metal^{n+}(H_2O)_x]$ of the clay surface. Such an extrinsic acidity corresponds to the second peak in a TPD patter, and is greatly influenced by the exchangeable cation. A bedeilite–montmorillonite mixture contains both $[([Si–O–Al]^{-})Metal^{+}(H_2O)_x]$groups belonging to bedeilitic tetrahedral Si-layer and $[([Al–O–Mn(Fe)]^{-})Metal^{+}(H_2O)_x]$ groups belonging to montmorillonitic octahedral Al-layer [9]. In nearly similar proportions, the TPD pattern should display two peaks instead of one (pure bedeilite or pure montmorillonite).

With increasing temperature, Brønsted acid sites progressively convert into Lewis ones, inducing, thereby, changes in the [Brønsted:Lewis] ratio [1,13,31,32]. Unless temperature is excessively increased, dehydroxylation still remains reversible. Beyond 350 °C, more or less pronounced clay dehydroxylation takes place. For a given clay sample, the [2 Brønsted $\leftrightarrows$ Lewis] equilibrium is greatly influenced by the exchangeable cation, and increasing temperature intensifies the differences in the chemical behaviors between the clay samples and in their TPD profiles. This is why homologous pairs of cations such as Na^+ and K^+ showed different profiles for both acidity and basicity. The same observations were made for Ca^{2+} and Mg^{2+}, or for transition bivalent cations.

4.3. Effects of the heating rate and gas flow rate

During TPD, desorption occurs unidirectionally, along the column axis x, and must obey the basic principles of adsorption chromatography theory [17], provided that time is replaced by temperature, like in programmed temperature gas chromatography [23], and to a lesser extent thermal differential analysis [24]. With increasing temperature, the released NH_3 or CO_2 molecules are randomly evacuated by the carrier gas stream, being more or less attracted by surface sites having various acid or base strengths. In their translations, these molecules are supposed to cross the column linearly so as all the velocity vectors can be assumed as being parallel (laminar flow or displacement). This assumption can be easily achieved with optimal operating particle size, heating rate, and carrier gas flow rate, when no convection and forced desorption take place. Thus, such interactions will rather be governed by thermodynamics than by kinetics. This makes the TPD peak to be perfectly symmetrical, displaying Gaussian shape.

The adsorption–desorption equilibrium depends on both temperature and throughput of the carrier gas. When no carrier gas is used, only thermal equilibrium is established between adsorbed and desorbed molecules. As the carrier gas throughput is raised, the desorbed molecules are increasingly evacuated, and equilibrium is progressively slightly displaced towards desorption. Raising even more the carrier gas throughput, the desorbed probe gas molecules acquire high velocities, and equilibrium disappears under forced desorption by convection. This phenomenon is more pronounced with increasing temperature. At the limit, a powerful flow rate of the carrier gas can cause pronounced desorption of the probe gas even at 100–200 °C. As a consequence, surface area of the TPD peak are markedly influenced, inducing errors in TPD measurements. This why attention must be paid in achieving the purge of the non-adsorbed probe gas excess at temperature lower than 50–80 °C, prior to TPD measurements.

5. Conclusion

A narrow dependence between the gas flow rate and the heating rate for a given porosity in the fixed bed has of clay samples been herein demonstrated. Analogy between TPD and thermal programmed gas chromatography can be achieved only at optimal [flow rate:heating rate] ratio, in fixed clay particle size.

The results obtained herein allow to conclude that the medium to strong acidity is induced by the exchangeable cation, while weak acidity and basicity are intrinsic features of the clay sheet framework. It was also found that there no exist pure acidic, pure base or neutral clay materials, since all clays displayed both acid and base characters, and that both acidity and basicity vary according to the exchangeable cation. By varying the exchangeable cation from alkaline to actinides, the total acidity of a clay sample increases with decreasing total base character of the anionic surface.

The most significant finding in the present work is that the acid strength increases at the expense of the base strength, and vice versa, in the same manner as in liquid. This similarity can be explained only in terms of polarizing effect and hydration grade of the exchangeable cation, and of similarity between solutions and condensed adsorbed state over the clay surface.

References

[1] A. Azzouz, E. Dumitriu, V. Hulea, C. Catrinescu, G. Carja, Prog. Catal. 5 (1) (1996) 9.
[2] R.J. Hunter, Foundations of Colloid Science, vol. 1, Oxford University Press, Oxford, 1995, p. 673.
[3] J.A. Davis, D.B. Kent, Surface complexation models in aqueous chemistry, reviews in mineralogy, in: M.F. Hochella, A.F. White (Eds.), Mineral Water Interface Geochemistry, vol. 23, Mineralogical Soc. Am., Washington, 1990, pp. 176–260.
[4] W. Stumm, J.J. Morgan, Aquatic chemistry, in: An Introduction Emphasizing Chemical Equilibria in Natural Waters, 3rd ed., John Wiley, New York, 1970, pp. 1022.
[5] F.M.M. Morel, J.G. Hering, Principles and Applications of Aquatic Chemistry, John Wiley, New-York, 1993, pp. 588.
[6] Surface complexation models in aqueous chemistry, reviews in mineralogy, in: M.F. Hochella, A.F. White (Eds.), Mineral Water Interface Geochemistry, vol. 23, Mineralogical Soc. Am., Washington, 1990, p. 603.
[7] H.H. Murray, Applied Clay Mineralogy Today and Tomorrow, Clay Miner. 34 (1999) 39–49.
[8] J.L. Venaruzzo, C. Volzone, M.L. Rueda, J. Ortiga, Micropor. Mesopor. Mater. 56 (2002) 73.
[9] A. Azzouz, D. Messad, D. Nistor, C. Catrinescu, A. Zvolinschi, S. Asaftei, Appl. Catal. A: Gen. 241 (2003) 1–13.
[10] J. Lyklema, Fundamentals of Interface and Colloid Science. I. Fundamentals, AC Press, London, 1991.
[11] T. Cseri, S. Bekassy, F. Figueras, S. Rizner, J. Mol. Catal. A: Chem. 98 (1995) 101.
[12] A. Azzouz, D. Nibou, B. Abbad, M. Achache, J. Mol. Catal. 68 (1991) 187.
[13] D. Barthomeuf, Acidity and Basicity in Zeolites, Stud. Surf. Sci. Catal. 65 (1991) 157.
[14] J. Xie, M. Huang, S. Kaliaguine, Catal. Lett. 29 (1994) 281.
[15] M. Huang, A. Adnot, S. Kaliaguine, J. Catal. 137 (1992) 322.
[16] L. Lapidus, N.R. Amundsen, Mathematic of adsorption in beds, vol. VI, J. Phys. Chem. 56 (1952) 984.
[17] J.A. Jönson, Chromatographic theory and basic principles, in: J.A. Jönson (Ed.), Chromatographic Science Series, Marcel Dekker, New-York, 1987, pp. 1–102.
[18] W.W. Yau, Anal. Chem. 49 (1977) 395.
[19] J.J. Van Deemter, F.J. Zuiderweg, A. Klinkenberg, Chem. Eng. Sci. 5 (1956) 271.
[20] H. Purnell, Gas Chromatography, Wiley, New-York, 1962, pp. 10–45.
[21] E. Grushka, J. Phys. Chem. 76 (1972) 2586.
[22] B. Ravindranath, Principles and Practice of Chromatography, Ellis Horwood Ltd. Publishers, Chichester, 1989, p. 74.
[23] L. Szepesy, E.D. Morgan, Gas Chromatography, Publishing House of the Hungarian Academy of Sciences, Budapest, 1970, pp. 272–281.
[24] A.P. Rollet, R. Bouaziz, L'Analyse Thermique, Tome 1-Les changements de phase, in: Gauthier (Ed.), Collection Monographies de Chimie Minérale, Villars, Paris, 1972.
[25] S. Bodoardo, R. Chiappetta, B. Onida, F. Figueras, E. Garrone, Proceedings of the III Convegno Nazionale Di Scienza Delle Zeoliti, Cetraro, Italy, September 28–29, 1995.
[26] B.M. Choudary, M. Sateesh, M.L. Kantam, K.M.V.R. Prasad, Appl. Catal. A: Gen. 171 (1998) 155.
[27] G. Mao, M. Tsuji, Y. Tamaura, Clays Clay Miner. 41 (1993) 731.
[28] T. Yamagishi, W. Ogasawara, E. Narita, Clay Sci. 11 (1999) 1.
[29] R.M. Barrer, R.M. Gibons, Trans. Faraday Soc. 61 (1965) 948.
[30] C.-C Su, Y.-H. Shen, Colloids Surf. A: Physicochem. Eng. Aspects 259 (2005) 173.
[31] M.G. Neumann, F. Gessner, C.C. Schmitt, R. Sartori, J. Colloid Interf. Sci. 255 (2002) 254.
[32] G. Aguilar-Armenta, G. Hernandez-Ramirez, E. Flores-Loyola, A. Ugarte-Castenada, R. Silva-Gonzalez, C. Tabares-Munoz, A. Jimenez-Lopez, E. Rodriguez-Castelon, J. Phys. Chem. B 105 (2001) 1313.